Article

Current Biology

Leaf dissection and margin serration are independently regulated by two regulators converging on the CUC2-auxin module in strawberry

Graphical abstract

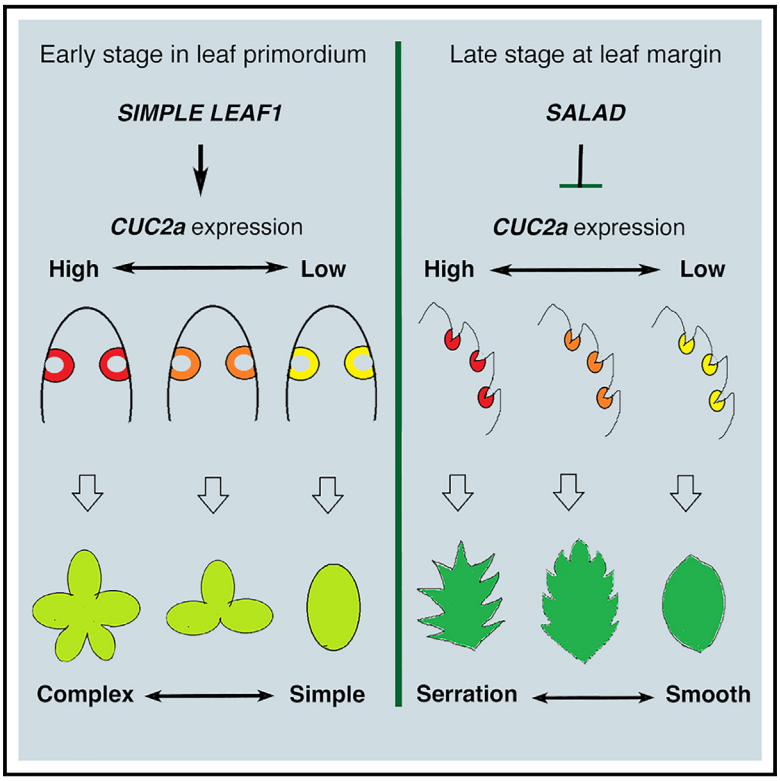

Authors

Xi Luo, Lei Guo, Ethan Tagliere, Zhenbiao Yang, Zhongchi Liu

Correspondence

zliu@umd.edu

In brief

Using the wild strawberry as a model, Luo et al. illustrate how two transcription factors, *SIMPLE LEAF1* and *SALAD*, regulate leaf complexity and leaf margin serration, respectively, through modulating *CUC2a* expression in distinct temporal and spatial domains of leaf primordia.

Highlights

- Leaf serration is regulated by *SALAD*, a single-Myb domain protein in strawberry
- *CUC2a* regulates leaf complexity and serration at different stages of leaf primordia
- *SIMPLE LEAF1* (*SL1*) and *SALAD* regulate *CUC2a* independently at leaf primordia
- Knockouts of both *SALAD* homologs in *Arabidopsis* also lead to deeper leaf serration

Luo et al., 2024, Current Biology *34*, 769–780
February 26, 2024
https://doi.org/10.1016/j.cub.2024.01.010

CellPress

Current Biology

CellPress

Article

Leaf dissection and margin serration are independently regulated by two regulators converging on the CUC2-auxin module in strawberry

Xi Luo,[1] Lei Guo,[1] Ethan Tagliere,[1] Zhenbiao Yang,[2] and Zhongchi Liu[1,3,4,*]
[1]Department of Cell Biology and Molecular Genetics, University of Maryland, College Park, MD 20742, USA
[2]Key Laboratory of Quantitative Synthetic Biology, Shenzhen Institute of Synthetic Biology, Shenzhen Institutes of Advanced Technology, Chinese Academy of Sciences, Shenzhen 518055, China
[3]X (formerly Twitter): @Berrylab_UMD
[4]Lead contact
*Correspondence: zliu@umd.edu
https://doi.org/10.1016/j.cub.2024.01.010

SUMMARY

The remarkable diversity of leaf forms allows plants to adapt to their living environment. In general, leaf diversity is shaped by leaf complexity (compound or simple) and leaf margin pattern (entire, serrated, or lobed). Prior studies in multiple species have uncovered a conserved module of *CUC2*-auxin that regulates both leaf complexity and margin serration. How this module is regulated in different species to contribute to the species-specific leaf form is unclear. Furthermore, the mechanistic connection between leaf complexity and leaf serration regulation is not well studied. Strawberry has trifoliate compound leaves with serrations at the margin. In the wild strawberry *Fragaria vesca*, a mutant named *salad* was isolated that showed deeper leaf serrations but normal leaf complexity. *SALAD* encodes a single-Myb domain protein and is expressed at the leaf margin. Genetic analysis showed that *cuc2a* is epistatic to *salad*, indicating that *SALAD* normally limits leaf serration depth by repressing *CUC2a* expression. When both *Arabidopsis* homologs of *SALAD* were knocked out, deeper serrations were observed in *Arabidopsis* rosette leaves, supporting a conserved function of *SALAD* in leaf serration regulation. We incorporated the analysis of a third strawberry mutant *simple leaf 1* (*sl1*) with reduced leaf complexity but normal leaf serration. We showed that *SL1* and *SALAD* independently regulate *CUC2a* at different stages of leaf development to, respectively, regulate leaf complexity and leaf serration. Our results provide a clear and simple mechanism of how leaf complexity and leaf serration are coordinately as well as independently regulated to achieve diverse leaf forms.

INTRODUCTION

Eudicot leaves exhibit tremendous morphological diversity, which impacts many aspects of plant physiology, including thermoregulation and hydraulic efficiency, and contributes to plants' adaptation to the environment.[1] The diversity of leaves is mainly determined by two factors: the leaf complexity and leaf margin features. The leaf complexity can be categorized as simple leaf, composed of a single flat lamina, or compound leaf, composed of multiple simple-leaf-like leaflets. The compound leaves could be pinnate, where pairs of leaflets are formed along the rachis, or palmate, when all leaflets initiate from the endpoint of a petiole.[2] The leaf margin, however, can be entire, serrated, or lobed with varying degrees of serration depth.[3]

Comparative and evolutionary studies revealed that compound leaves repeatedly arose from simple-leaved ancestors and could evolve through distinct mechanisms.[2] In simple leaf species such as *Arabidopsis* and maize, the class I *KNOTTED-LIKE-HOMEOBOX* (*KNOX*) gene is expressed in the shoot apical meristem but absent from the incipient leaf primordia. By contrast, in compound leaf species such as tomato and *Cardamine hirsuta*, *KNOXI* expression reappears in the young leaf primordia to stimulate new leaflet primordia formation.[4–6] The difference in *KNOXI* expression patterns between simple and compound species suggests distinct genetic programs underlying primary (simple) leaf vs. compound leaf development.[7] Indeed, although overexpressing *KNOXI* causes compound leaves of tomato or *C. hirsuta* to produce even more leaflets and higher order leaflets, overexpressing *KNOXI* failed to cause the simple leaves of *Arabidopsis*, tobacco, and the tomato *La* mutants to become compound.[5–8] *KNOXI* appears to function by delaying leaf primordial differentiation and stimulating leaf-wide growth.[9,10]

However, not all species rely on *KNOXI* for compound leaf development. In a subclade of *Fabaceae*, the inverted-repeat lacking clade (IRLC), *KNOXI* gene expression is absent from the compound leaf primordia. Instead, the *UNIFOLIATA* in *Pisum sativum* and *SINGLE LEAFLET1* in *Medicago truncatula*, both orthologs of *LEAFY* (*LFY*) in *Arabidopsis*, are expressed in the leaf primordia and promote compound leaf development in place of *KNOXI*.[11–13]

In contrast to *KNOXI* and *LFY*, *Cup-shaped cotyledon* (*CUC*) genes, belonging to the *No Apical Meristem* (*NAM*) transcription factor family, appear to possess a conserved function for leaf complexity and leaf margin regulation in eudicot. *CUC* genes were initially identified in *Arabidopsis* because their mutants were defective in organ separation in cotyledons and floral organs.[14] *CUC* genes were later found to play a conserved role in leaflet separation in compound leaf species and leaf margin sinus formation in simple as well as compound leaf species.[3,15,16] In simple-leaved *Arabidopsis*, *CUC* overexpression caused more and deepening sinuses at the leaf margin, whereas *cuc* loss of function caused smooth leaf margins.[3,17,18] *CUC* similarly impacts leaf margin features in *C. hirsuta* and *Solanum lycopersicum*.[15] In compound leaf species, *CUC* marks the boundaries between leaflets and is required for leaflet separation in both *KNOXI*-dependent tomato and *LFY*-dependent *P. sativum* compound leaves.[15,19] Therefore, leaf margin serration and leaflet separation in compound leaves share a common mechanism involving *CUC*.

CUC interacts with auxin to regulate leaf complexity and margin features. Auxin maxima, organized by the auxin efflux carrier *PIN1*, was shown to localize at the tip of protruding leaflet or leaflet margin teeth. At the same time, the *CUC* was shown to be expressed in the group of cells surrounding the protrusions to locally repress cell proliferation. Thus, auxin and *CUC* shape the leaf margin by locally increasing growth at protrusions and decreasing growth at their flanks, respectively. These dynamic *CUC* and auxin expression patterns at the leaf margin are the result of a feedback regulatory loop via *PIN1* and *miR164*, a negative regulator of *CUC*, and together, they create differential growth between adjacent groups of cells.[16,19]

The existence of *KNOXI*-dependent and -independent mechanisms in different compound leaf species suggests that compound leaves may arise through employing different regulators that interact with the conserved *CUC*-auxin module. Therefore, expanding our investigations into other compound leaf species may help identify previously unknown regulators, clarify existing complexity, and broaden our understanding in the evolution of diverse leaf forms. Further, although the conserved *CUC*-auxin pathway is employed in both leaflet separation and leaf margin serration, what distinguishes their roles in these two developmental contexts is not known.

Wild diploid strawberry (*Fragaria vesca*) is a new model for investigating mechanisms of leaf morphology and diversity. The adult leaves of strawberry (*Fragaria* spp.) develop palmate compound leaves consisting of three leaflets, and each leaflet margin has well-defined serrations. Based on previous work, neither *KNOXI* nor *LFY* appeared to contribute in a major way to its leaf complexity regulation. RNAi-knockdown of *FaKNOX1* did not reduce leaf complexity; in *fvelfy*a mutants, only a small percentage of leaves showed smaller leaflets, or in extreme cases, reduced leaflet number from three to two.[20,21] Furthermore, overexpression of *FaKNOX1* did not increase leaf complexity and only resulted in severely dwarf plants with wrinkled and curled leaves.[20] One possible explanation is that strawberry compound leaf formation differs from the well-studied compound-leaved species, tomato, *C. hirsuta*, and legume. Alternatively, a different strawberry *KNOXI* gene (yet to be identified) may perform the function in leaf complexity regulation. Regardless, *F. vesca* provides a new opportunity to investigate leaf morphogenesis.

Recently, a new mutant, *simple leaf 1* (*sl1*), was found in *F. vesca* that develops simple leaves instead of trifoliate leaves. This *sl1* mutation is allelic to an 8 bp deletion found in *Fragaria vesca* "*monophylla*," which is a simple leaf strawberry variety raised by Duchesne in Versailles in 1761. The reduced leaf complexity of *sl1* and *monophylla* was caused by mutations in a novel gene encoding a transcription factor with DNA binding GT-1 and protein kinase PKc domains.[22] In addition, the conserved *FvemiR164-FveCUC2a* module was also identified and characterized in *F. vesca*. Consistent with the idea of *CUC2a* as a conserved regulator of leaf morphology, *fvecuc2a* mutants exhibited reduced leaf complexity due to leaflet fusion and smooth leaf margin due to a lack of serration.[23] These prior studies provide us a strong foundation for investigating leaf morphological diversity using *F. vesca* as a model.

In this study, we identified a deep-serrated leaf mutant in *F. vesca* from an ethyl methanesulfonate (EMS) mutagenesis screen. The mutant, named *salad*, was shown to result from a mutation in a single-MYB (myeloblastosis) domain transcription factor gene and has a defect specifically in the leaf margin without affecting leaf complexity. Using CRISPR-Cas9 to simultaneously knock out both homologs of *SALAD* in *Arabidopsis*, the resulting *Arabidopsis* double mutant showed more and deeper margin serrations in the rosette leaves, suggesting that *SALAD* encodes a conserved regulator that acts to limit leaf margin indentation. Further, *SALAD* was shown to be an upstream regulator of *FveCUC2a*, whose upregulation in the *salad* mutants was responsible for the deep margin serration phenotype. To investigate the relationship between leaf complexity regulated by *SL1* and leaf margin serration by *SALAD*, we constructed *F. vesca* double mutants among *sl1-monophylla*, *fvecuc2a*, and *salad*, which showed that the process of leaf complexity and leaf serration is regulated by two genetically independent pathways defined by *SL1* and *SALAD*, respectively. These two pathways converge upon *FveCUC2a* at different stages of leaf development. By investigating the mechanism of compound leaf development in strawberry, we gain insights into the mechanism and relationship between leaflet separation and leaf margin serration formation as well as how the identified novel regulators *SALAD* and *SL1* interact with the conserved *CUC*-auxin regulatory module.

RESULTS

The *SALAD* locus regulates leaf serration depth in *F. vesca*

A *F. vesca* mutant with a short stature and deeper leaf serration was identified in an EMS mutagenesis screen of "Yellow Wonder (YW5AF7)" accession (see STAR Methods). The mutant was named *salad* because of its resemblance to leafy greens in a salad. In wild-type (WT) *F. vesca*, the adult leaf is trifoliate with one terminal leaflet flanked by two lateral leaflets (Figures 1A and 1C). Each leaflet has moderate serrations (Figure 1C). The leaves of *salad* on the other hand are smaller and have deeper serrations, although they are still trifoliate (Figures 1B and 1D). Further, the number of serrations of each leaflet, terminal or lateral, is similar to that of WT leaflets (Figure 1E), suggesting

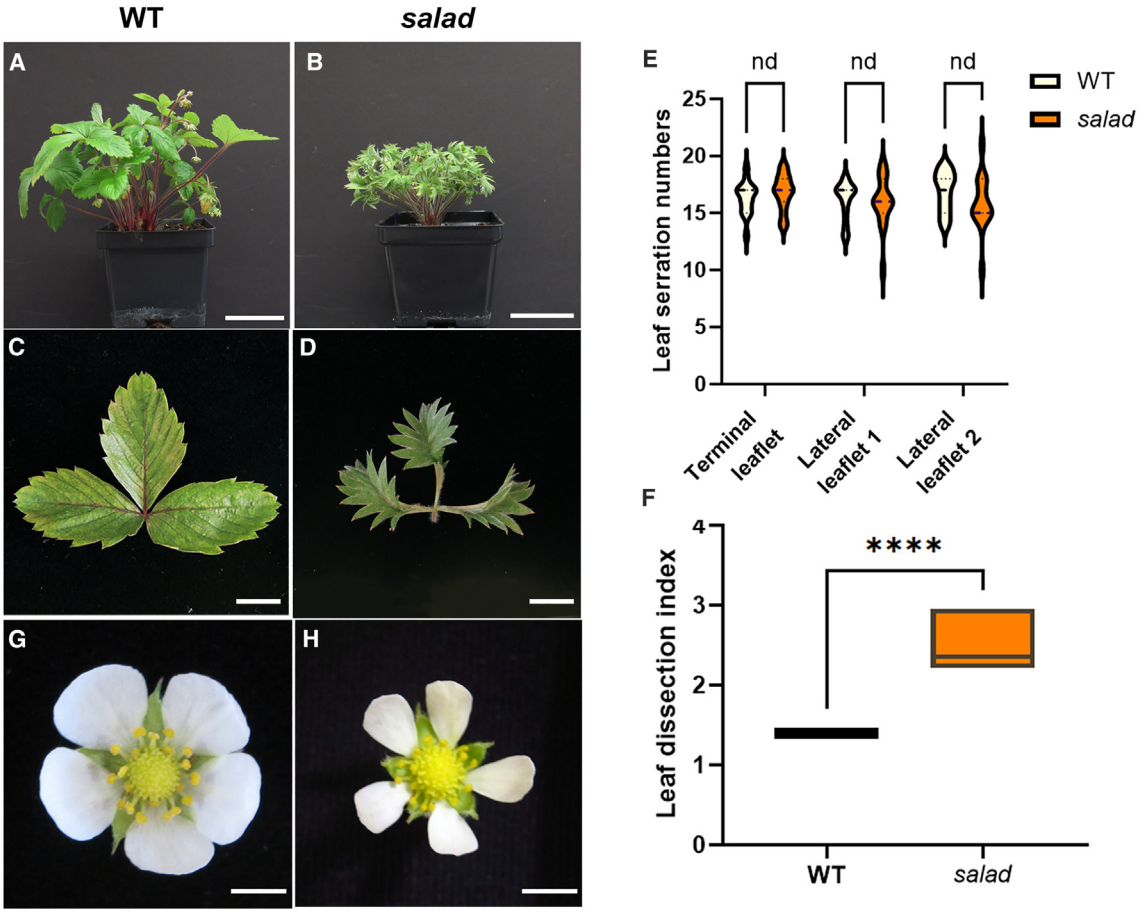

Figure 1. Characterization of *salad* mutant in *F. vesca*

(A–D) Whole plant and adult leaf of WT (YW5AF7) (A and C) and *salad* mutant (B and D).

(E) Quantification of serration number of three leaflets in WT and *salad*; data are means ± SD, n = 15. nd, not a discovery ($q \geq Q$), multiple t test corrected by false discovery rate (FDR) method.

(F) Leaf dissection index (LDI) of the terminal leaflet. LDI was calculated as leaf perimeter/square root of leaf area, n = 15. ****$p < 0.0001$, Student's t test, data are means ± SD.

(G and H) Flower phenotype of WT (G) and *salad* (H).

Scale bars, 5 cm in (A) and (B), 1 cm in (C) and (D), 5 mm in (G) and (H).

that *salad*'s leaf defect is limited to the depth of the serration. The leaf shape can be quantified by the variable leaf dissection index (LDI). Typically, an entire (smooth margin) leaf has an LDI value slightly larger than 1, and deeper lobed or serrated leaves have higher values.[24] In the WT, the LDI of the terminal leaflet is 1.40 ± 0.04, but the *salad* mutant has an LDI of 2.45 ± 0.24 (Figure 1F), suggesting a significant increase in serration depth. Beside the leaf serration, the *salad* mutant leaves are thicker and darker green, and the mutant flowers are smaller and have narrower petals (Figures 1G and 1H).

Mapping by sequencing maps *salad* to a single-MYB domain transcription factor

To identify the gene defined by *salad*, a mapping population was constructed by crossing *salad* with the WT accession "Hawaii 4 (H4)." Although all F1 plants resemble WT in phenotype, F2 segregated 31 *salad* mutants and 88 WT-looking plants. Thus, the *salad* phenotype is controlled by a single recessive mutation. Genomic DNA from 25 F2 *salad* mutants and 25 F2 phenotypically WT plants was separately pooled and sequenced. Using the SIMPLE pipeline,[25] the mutation was narrowed down to a 600 kb region on chromosome 4 (Figure S1). Among the 16 SNPs affecting 11 candidate genes (Table S1), 14 caused missense and 2 resulted in premature stop in 2 different genes. One such candidate gene has no annotation, and the other is GDR: FvH4_4g35980, encoding a single-MYB domain transcription factor (Figure 2A).

To determine if GDR: FvH4_4g35980 corresponds to *SALAD*, CRISPR-Cas9 was used to knock out GDR: FvH4_4g35980 in the WT parent (YW5AF7). Two single-guide RNAs (sgRNAs) targeted the first and third exon of GDR: FvH4_4g35980, respectively (Figure 2A). Five transgenic plants at the T1 generation showed the same phenotype as *salad* (Figures 2C and 2E). Sanger sequencing showed homozygous (−1, −1) and (+1, +1), or biallelic (+11, +1) edits in GDR: FvH4_4g35980 (Figure 2F). Taken together, the CRISPR knockouts confirm that GDR: FvH4_4g35980 is *SALAD*.

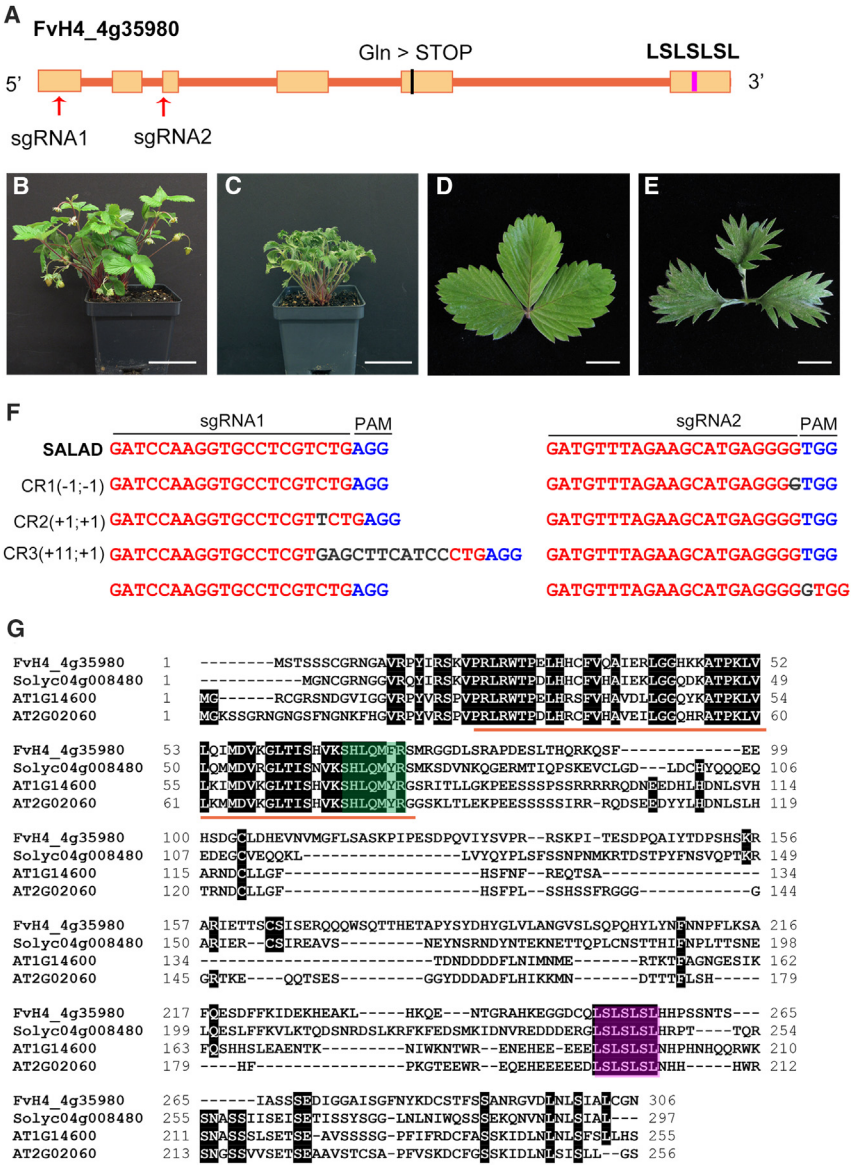

Figure 2. *SALAD* encodes a single-MYB motif transcription factor

(A) Schematic representation of the gene structure of *SALAD* (GDR: FvH4_4g35980). Orange boxes represent the exons, and scale bars represent the introns. The pink box represents the EAR motif. The vertical black line marks the mutation in the original *salad* mutant. The red arrows point to sgRNAs sequences. Also see Figure S1 and Table S1.

(B–E) Whole plant and mature leaf phenotype of WT (B and D) and *salad* ^{CR1} (C and E).

(F) CRISPR-Cas9-generated mutant alleles of *SALAD*. Red font indicates the sgRNA; gray font indicates insertions; – and + indicate deletion and insertion, respectively; and blue font indicates the protospacer adjacent motif (PAM).

(G) Multiple sequence alignment of protein sequences of SALAD and its homologs from *Solanum lycopersicum* (SGN: Solyc04g008480) and *Arabidopsis thaliana* (TAIR: AT1g14600, AT2g02060). The red line underlines the single-MYB domain. SHLQM [Y/F] residues are shaded with green; EAR motifs are shaded with purple.

Scale bars, 5 cm in (B) and (C) and 1 cm in (D) and (E).

SALAD encodes an SH[AL]QKY[RF]-class MYB transcription factor; the MYB domain is located at the N terminus of the protein. We identified the orthologs of *SALAD* in *Arabidopsis* and tomato (*S. lycopersicum*) by blasting and sequence alignment (Figure 2G). The overall sequence identity is between 24.1% and 31.1%. The MYB domain shares an identity of 77.8%–83.3%, whereas other regions have little conservation (Figure 2G). The SHLQMF motif in *F. vesca* is SHLQMY in tomato and *Arabidopsis*. An ethylene-responsive element binding factor-associated amphiphilic repression (EAR) motif, a conserved repression motif, is also found at the C terminus of this class of proteins. The ortholog of *SALAD* in tomato is the *CLAUSA* gene[26]; *clausa* loss-of-function mutants exhibited higher order of leaf complexity, deeper leaf margin serration, epiphyllus inflorescences, and navel-like fruits.[27] Hence, tomato mutants of *CLAUSA* appear to have a broader range of defects than the strawberry *salad* mutants.

fvecuc2a is epistatic to *salad* in regulating leaf margin serration

As *CUC2* encodes a conserved regulator of leaf margin, we examined the relationship between *salad* and *fvecuc2a* in *F. vesca*. In the single loss-of-function *fvecuc2a* mutant, the leaf margin became smooth and was completely devoid of serration. However, when the *FveCUC2a* transcript was stabilized in the absence of an *miRNA164*, the leaves became deeply serrated.[23] Therefore, in strawberry, *FveCUC2a* appears to promote leaf margin serration, which is opposite of *SALAD* that acts to limit leaf margin serration. We set out to construct the *salad; fvecuc2a-2* double mutant to test whether *SALAD* regulates *FveCUC2a*. A proportion of *fvecuc2a* homozygous mutants arrested at cotyledon stage with fused cotyledon and a loss of shoot apical meristem, and this phenotype was even more severe in the double mutants with majority seedling lethal. Therefore, we tissue-cultured F2 seedlings with fused cotyledons and successfully recovered a double mutant of *salad; fvecuc2a-2*. The double mutant produced small, narrow, and simple leaves with a smooth leaf margin that resembled *fvecuc2a-2* single mutants (Figure 3A). On the other hand, the dark green hairy leaves of the double mutant resembled those of the *salad* single mutant (Figure 3A). The observation that *fvecuc2a-2* is epistatic to *salad* in regulating leaf margin serration strongly supports that *SALAD* acts through *FveCUC2a* to limit leaf serration depth.

SALAD regulates leaf serrations by repressing *FveCUC2a*

Because of the MYB and EAR domains, *SALAD* could encode a transcriptional repressor and inhibit leaf margin serration by

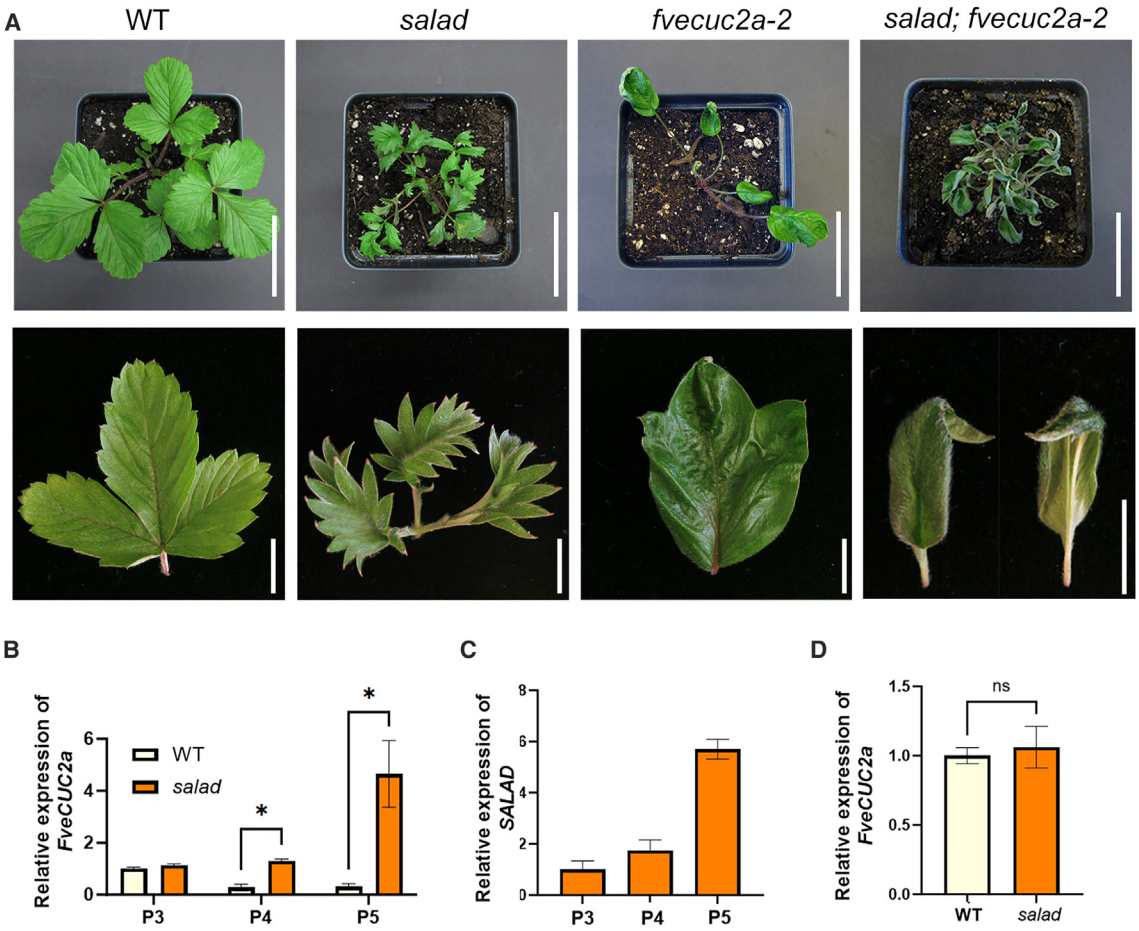

Figure 3. *SALAD* regulates leaf serration through repressing *FveCUC2a* transcription

(A) Epistasis analysis between *salad* and *fvecuc2a-2*. Plants and mature leaves of WT, *salad*, *cuc2a-2*, and *salad cuc2a-2*.

(B) RT-qPCR analysis of *FveCUC2a* mRNA expression level in wild-type and *salad* mutant at successive stages of early leaf development (P3–P5). *q < Q, multiple t test corrected by FDR method. Also see Figure S2.

(C) RT-qPCR analysis of *SALAD* transcript levels at successive stages (P3–P5) of early leaf development.

(D) RT-qPCR analysis of *FveCUC2a* transcript levels in WT and *salad* mutant in combined tissues (meristem to P2), ns, not statistically significant, Student's t test. Data are mean ± SD obtained from three technical replicates. The experiment was repeated three times with similar results.

Scale bars, 5 cm for the plants and 1 cm for the leaves in (A).

repressing *FveCUC2a* transcription. Quantitative reverse-transcription PCR (RT-qPCR) was performed to quantify *FveCUC2a* transcript level in the young leaves of WT and *salad* mutants. In strawberry, the serration emerges soon after leaflet separation when the leaf progresses to the P3 stage. Leaf primordia of P3, P4, and P5 stages were collected for RNA extraction. RT-qPCR showed that *FveCUC2a* expression gradually decreases from P3 to P5 in the WT but increases from P3 to P5 in the *salad* mutant (Figure 3B). Meanwhile, *SALAD* transcripts gradually increase from P3 to P5 in WT (Figure 3C), showing a negative correlation in expression trend with *FveCUC2a*. The RT-qPCR results support a negative regulation of *FveCUC2a* by *SALAD*.

We also attempted to examine the expression of *FveCUC2a* at earlier stages of leaf development. At P2, the leaf primordium is developing and subdividing into three leaflet primordia, leading to a compound leaf (Figure 4).[22] Yet, at the P2 stage, the leaf margin serration has not emerged. Due to its small size, we isolated shoot apex that contains shoot apical meristems together with P2 or younger stage leaf primordia. The *FveCUC2a* expression level in WT and *salad* was similar (Figure 3D), suggesting that *SALAD* may not have a role in leaflet initiation and may only act at later stages (P3 and onward) to repress *FveCUC2a* expression at the leaf margin. The repression of *FveCUC2* by SALAD is likely indirect, as we failed to see a direct repression of the *FveCUC2apro*::*LUC* reporter in a transient luciferase assay in tobacco (Figure S2).

Leaf morphogenesis is under precise regulation, and many key regulators have unique spatial-temporal expression patterns.[10,16,28] Figure 4A illustrates the early developmental process of *F. vesca* leaves based on published scanning electron microscopy (SEM).[22] Soon after the leaf primordium initiates from the shoot apical meristem, the tip of the primordium protrudes to initiate the terminal leaflet, whereas the two flanking "shoulders" become the lateral leaf primordia (P1).

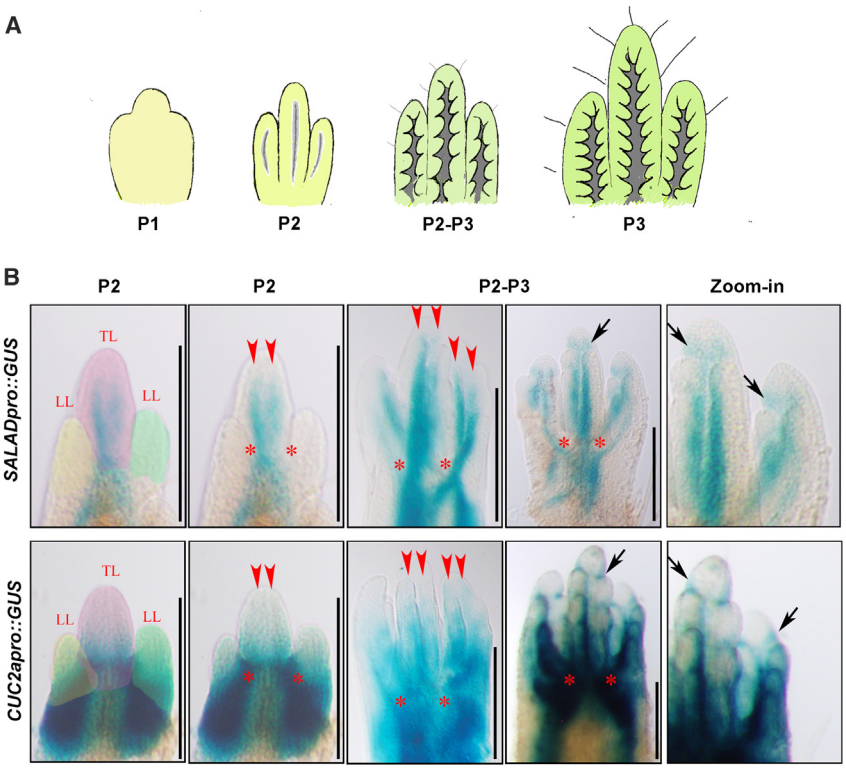

Figure 4. *SALAD* expression overlaps with *FveCUC2a* expression at the leaf serration sinus

(A) Illustration of leaf morphology from developmental stages P1 to P3 based on published SEM images.[22]

(B) *SALADpro::GUS* and *CUC2apro::GUS* expression in developing leaf primordia. Red asterisk (*) denotes the base between leaflets, red arrowheads point to the margins of the leaflets, and black arrows point to the sinus of serrations. (LL, lateral leaflet; TL, terminal leaflet.)

Scale bars, 200 μm in (B).

Subsequently at P2 stage, the terminal and the two lateral leaflet primordia elongate distally, and the adaxial side of each leaflet sinks to create a rolled-in leaflet. At P3, the leaflet margin shows serrations, and the leaf abaxial side is covered with trichomes. Ultimately, each leaflet will expand, unfold, and elongate to a mature leaflet.

To examine more precisely the dynamic spatial and temporal expression patterns of *SALAD* and *FveCUC2a* during leaf morphogenesis, GUS reporter lines were generated, respectively. A 2,154 bp *SALAD* promoter driven GUS construct *SALADpro::GUS* was transformed into YW5AF7, and 12 transgenic plants were obtained. Young leaf primordia from P2 to P3 were collected and stained with X-gluc (Figure 4B). At P2, the *SALADpro*::GUS signal was present as two strips (see the red arrowheads) in the center of the terminal leaflet, where the leaf margins were initiating. Later (P2 and P3), the margins of lateral leaflets became visible and coincided with the appearance of two strips of GUS signal in the center of lateral leaflets (red arrowheads in P2 and P3 Figure 4B). As the leaflet progressed to P3, GUS signal was confined to the base of the serrations, more specifically at the sinus of the serrations (black arrows in Figure 4B), showing a discontinuous distribution. In addition to its expression in the leaf margin, *SALADpro::GUS* signal was also detected in the vasculature. The result suggested that *SALAD* is mainly expressed at the leaf margin, where serrations initiate, and later at the sinus to regulate serration depth.

We also generated 14 lines of transgenic plants expressing the *FveCUC2apro::GUS* reporter, which allowed us to compare the expression pattern of *FveCUC2apro::GUS* with that of *SALADpro::GUS*. At P2, *FveCUC2apro:: GUS* signal was most intense in the base between leaflets (red "*"; Figure 4B). When serrations started to form at the leaf margin (red arrowheads, P2 and P3), the GUS signal was visible both between leaflets (red "*", Figure 4B) and at the sinuses of serrations (black arrows; Figure 4B). The result is consistent with a function of *CUC2a* in promoting separations between leaflets as well as between leaf margin serrations.[23] The *FveCUC2apro::GUS* expression overlaps with the expression of *SALADpro::GUS* at the leaf serration sinus at stages P2 to P3 (Figure 4B), supporting that *SALAD* may regulate *FveCUC2a* expression starting as early as the P2 to P3 stages when leaflet margins start to form serrations. However, *FveCUC2a* is distinctly expressed between the leaflet primordia at P2 (red "*", Figure 4B), which corresponds with its earlier role in leaflet separation and is likely independent of *SALAD*.

The role of auxin at the leaf margin

It is well established that *CUC2* functions by patterning the discrete leaf marginal auxin maxima, which mark the protrusions of the serrations.[16] Since *FveCUC2a* expression is increased in *salad* mutants (Figure 3B), the auxin level or distribution at the leaflets may be altered. Therefore, we introduced a *F. vesca DR5ver2::GUS* auxin response reporter[29] into *salad* through crossing. GUS staining was performed during leaflet and serration initiation (Figure 5A). Consistent with the previous findings in other species,[9,16] auxin maximum was observed at the protrusions of leaflet primordia at P2 stage (black arrow in Figure 5A) and discrete leaf margin protrusions at the late P2 to early P3 stage (black arrowhead in Figure 5A) in WT. This *DR5ver2::GUS* expression pattern was similar in *salad* mutants (Figure 5A), suggesting that auxin distribution is unchanged in *salad* mutants. To test if auxin level is changed, RT-qPCR was conducted to measure *GUS* transcript levels in the shoot tips of *DR5ver2::GUS* plants, including the shoot meristem plus young leaf primordia from P1 to P4. The *GUS* transcripts in *salad* mutants were significantly higher than that in WT (Figure 5B), indicating a higher auxin level in *salad* mutants.

We also tested whether the deep serration phenotype could be mimicked by applying auxin (naphthaleneacetic acid, NAA) to the WT plants. NAA treatment didn't change leaf margin nor leaf complexity in NAA treated plants (Figure 5C), suggesting that simply increasing auxin level is insufficient to induce

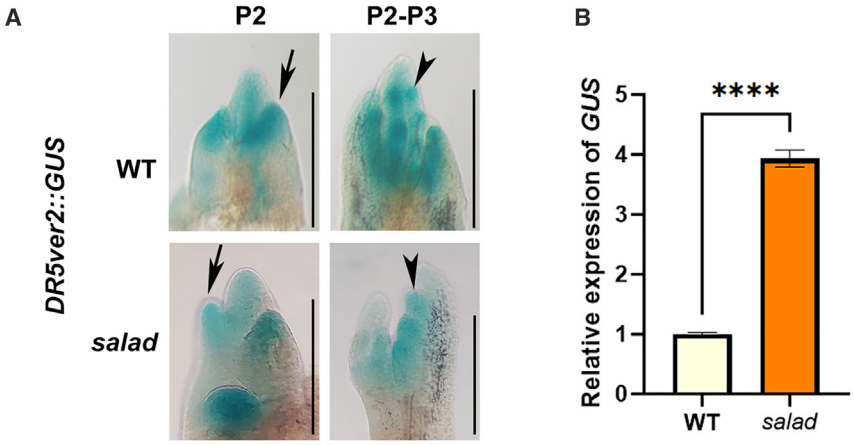

Figure 5. *SALAD* regulates serration depth through auxin

(A) *DR5ver2::GUS* expression in the developing leaf primordia of WT and *salad*. Black arrows indicate auxin maximum at the leaflet primordia, and black arrowheads indicate discrete auxin maximum along the leaf margin.

(B) RT-qPCR analysis of *DR5ver2::GUS* reporter expression in WT and *salad* shoot apices (shoot meristem plus up P4). ****$p < 0.0001$, Student's t test. Data are mean ± SD obtained from three technical replicates.

(C) Leaves of WT and *salad* treated by mock, NAA (1 μM), or NPA (20 μM).

Scale bars, 200 μm in (A) and 0.5 cm in (C).

deeper serrations or leaf complexity. We then tested if blocking auxin transport with N-1-naphthylpthalamic acid (NPA) could reverse the *salad* phenotype. Both WT and *salad* plants started to produce simple leaves without any or with very few serrations after NPA treatment (Figure 5C). These results are consistent with a role of auxin transport in creating the auxin maxima, which, together with *CUC2*, is needed to generate the differential growth between sinuses and protrusions during leaf morphogenesis. The data also suggests that *SALAD* acts upstream to modulate the feedback regulatory loop consisting of *FveCUC2a* and *FvePIN1*.

SALAD orthologs in *Arabidopsis* also regulate leaf serration

CUC2 has a conserved function in patterning *Arabidopsis* leaf serration, as stabilized *CUC2* transcripts in the *Arabidopsis mir164a* null mutant led to deeper serrations.[30] If *SALAD* regulates leaf serration through repressing *FveCUC2* in strawberry, could *SALAD* play an evolutionarily conserved role in other plant species? We adopted the CRISPR-combo system[31] to simultaneously knock out the two *Arabidopsis* orthologs of *SALAD*, TAIR: *AT1G14600* and TAIR: *AT2G02060* (Figure 2G), to overcome functional redundancy. Three independent double mutants were obtained (Figure 6A). In the WT (Col-0), the proximal part of each simple leaf blade is more serrated than the distal part[30] (red arrows, Figure 6B). All three mutant lines showed deeper leaf serrations than the WT (red arrows, Figure 6B), and the phenotype resembled that of *CUC2* overaccumulation in the *Arabidopsis mir164a* mutants.[30] The result strongly suggests that the *SALAD* orthologs in *Arabidopsis* have a conserved function in regulating leaf margin serration depth, possibly through the repression of *CUC2*.

We also overexpressed *FveSALAD* in *Arabidopsis* to test if it would cause smooth leaf margins. *35S::FveSALAD* was transformed into *Arabidopsis*. Seven independent *FveSALAD-OE* lines were obtained, and the leaf morphology was similar to the WT (Figure 6B). Perhaps FveSALAD requires other co-factors to repress *CUC2*, or the less conserved regions of FveSALAD may determine its species-specific interactions with co-factors.

Leaf complexity and serration are separately regulated by *SL1* and *SALAD* through *FveCUC2a*

In *F. vesca*, the *sl1* mutants produce simple leaves instead of trifoliate compound leaves but the *sl1* leaves possess normal margin serrations (Figure 7A).[22] The respective effect of *sl1* and *salad* on leaf complexity and leaf margin serration provided an opportunity to investigate the relationship between these two processes. We constructed *salad*; *sl1-monophylla* double mutants, which showed an additive genetic interaction; they develop both simple leaves and deep serrations, indicating that *SALAD* and *SL1* act independently of each other to regulate leaf serration and leaf complexity, respectively (Figure 7A). *SL1* expression was detected in the entire primordium and overlapped with *FveCUC2a* expression at the boundaries between the leaflets during early stages of leaflet emergence. Later, *SL1* expression was confined to the tip of serrations

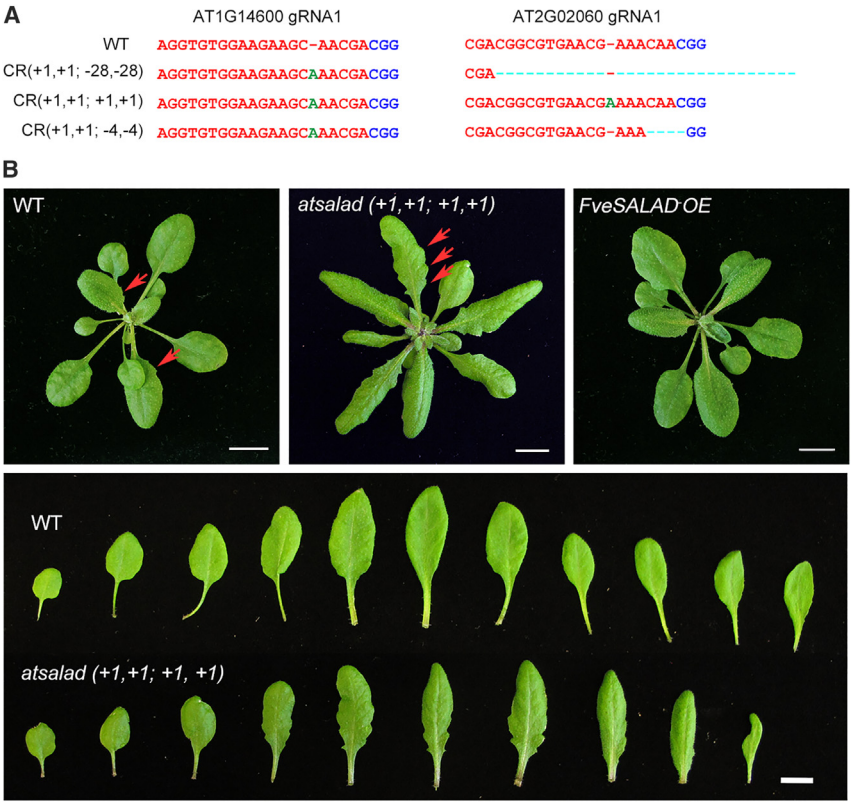

Figure 6. *SALAD* homologs in *Arabidopsis* also function in leaf margin serration

(A) CRISPR-Cas9-editted sequences in the two *SALAD* homologs, TAIR: *AT1G14600* and TAIR: *AT2G02060*, in *Arabidopsis*. Red font indicates the sgRNA sequence; green font indicates insertions; light blue font indicates deletions; – and + indicate deletion and insertion, respectively; blue font indicates the protospacer adjacent motif (PAM).

(B) Images of rosette (top) and rosette leaf series (bottom) of the WT (Col-0) and the *atsalad* double mutant. Top right is a *FveSALAD*-OE transgenic plant.

Scale bars, 1 cm.

(Figure 7C).[22] Therefore, we hypothesize that *SL1* may act at the early stages (P1 and P2) to promote *FveCUC2a* expression at the base of leaflets to facilitate leaflet separation. To test this hypothesis, we investigated *FveCUC2a* expression in *sl1-monophylla* and WT leaf primordia at P2 and P3 stages. Due to small size, we were unable to isolate P1 stage leaf primordia. RT-qPCR showed that *FveCUC2a* expression was significantly reduced in *sl1-monophylla* P2 and P3 leaf primordia when compared with WT (Figure 7B), indicating that SL1 activity is required to maintain high levels of *FveCUC2a* expression required for leaflet separation at the P2 and P3 stage leaf primordia.

DISCUSSION

In this study, we identified and characterized a *F. vesca* mutant *salad* with abnormally deeper serrations at the leaf margin. Using this mutant, we probed into the mechanism of leaf serration regulation, which led to the discovery of *SALAD* as a novel regulator of a highly conserved *FveCUC2a-FvePIN1* regulatory module in leaf morphogenesis. Based on genetic interactions and expression analysis, we demonstrated that *SL1* and *SALAD* regulate *FveCUC2a* expression independently and at different stages of leaf development. Specifically, *SL1* acts in P1-P2 leaf primordia to promote *FveCUC2a* expression at the base between leaflets (Figure 7C), which is required for compound leaf formation. By contrast, *SALAD* acts in P3-P4-P5 leaflet margin to repress *FveCUC2a* expression (Figure 7C) to limit sinus depth between serration protrusions. Therefore, our study showed that leaf complexity and leaf margin features could evolve independently by resorting to different regulatory proteins, *SL1* and *SALAD*, that converge upon a common downstream regulator *CUC2* at different spatial and temporal domains (Figure 7D). Further, through CRISPR-Cas9-knockout of SALAD's homologs in *Arabidopsis*, we showed that *SALAD* likely encodes a conserved regulator of leaf margin serration via its regulation of *CUC2*, highlighting the value of strawberry, a non-model, in uncovering novel regulators of conserved processes. Together, our study provided a simple mechanistic example of how involvement of independent regulators such as *SL1* and *SALAD* at different space and time could enable modifications of leaf complexity or leaf margin feature separately.

Strawberry offers an alternative system to investigate the role of *KNOXI* in compound leaf development

In compound-leaved tomatoes and *C. hirsuta*, overexpressing *KNOXI* (maize *KN1* or tomato *Tkn2*) produced higher order leaflets. By contrast, overexpressing *KNOXI* in simple-leaved *Arabidopsis*, tobacco, maize, and the tomato *La* mutant (which makes simple leaves) did not convert simple leaves to compound leaves, suggesting some intrinsic genetic mechanism distinguishing simple from compound leaves.[2,6–8] Recently, Challa et al.[32] showed that two classes of genes, the *CINCINNATA-like TEOSINTE BRANCHED1*, *CYCLOIDEA*, *PROLIFERATIVE-CELL FACTORS* (*CIN/TCP*), and *KNOXII* act redundantly in the simple leaves to prevent leaflet initiation. In *Arabidopsis*, simultaneous downregulation of *CIN-TCP* and *KNOXII* led to the reactivation of *KNOXI* and *CUC*, which caused repeated leaflet initiation and super-compound leaves.

Previously, overexpression of a *KNOXI* gene from cultivated strawberry *Fragaria* × *ananassa* (*FaKNOX1*) in wild diploid strawberry *F. vesca* did not increase higher order leaves.[20] One interpretation is that *FaKNOX1* is not orthologous to the maize *KN1* or tomato *Tkn2* and hence couldn't cause higher order leaflet formation in *F. vesca*. To identify the true ortholog of maize *KN1*, we constructed a phylogenetic tree using KNOX proteins from *F. vesca*, *Arabidopsis*, tomato and also included FaKNOX1 and maize KN1 (Figure S3). The phylogenetic tree shows three

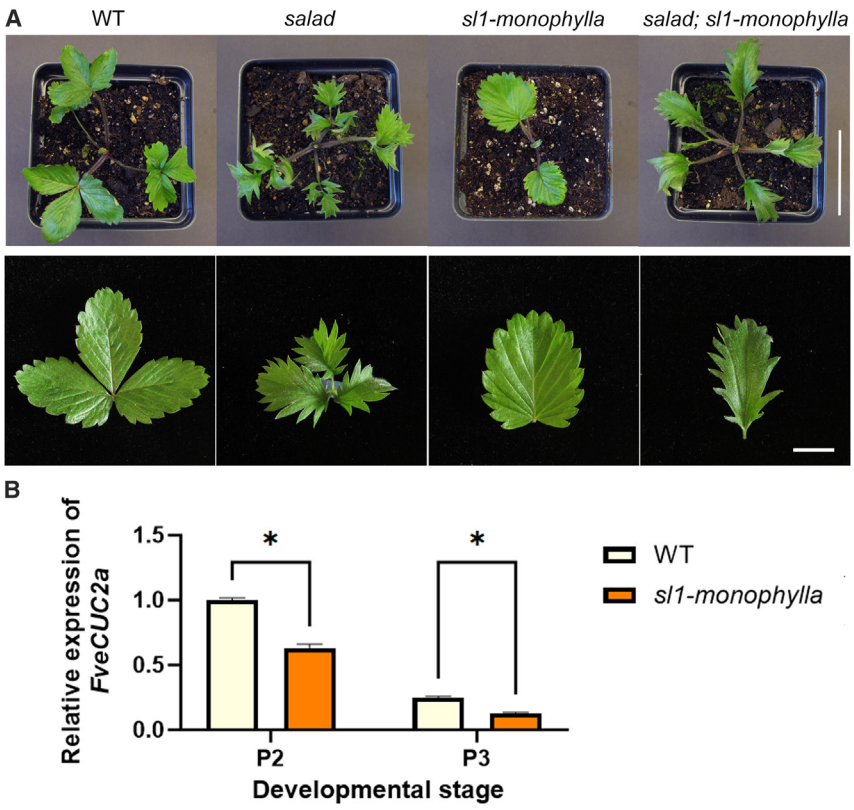

Figure 7. *SL1* and *SALAD* independently and, respectively, regulate leaf complexity and serration

(A) Genetic analysis between *salad* and *sl1-monophylla*. Plants and mature leaves of WT, *salad*, and *sl1-monophylla* single and *salad; sl1-monophylla* double mutants.

(B) RT-qPCR analysis of *FveCUC2a* transcript levels in WT and *sl1-monophylla* in P2 and P3 leaves. *$p < 0.01$, Student's t test. Data are mean ± SD obtained from three technical replicates.

(C) Diagrams showing the expression of *FveCUC2a*, *SALAD*, and *SL1* in P2 and P3 stage leaves. At P2, *SL1* and *FveCUC2a* expression overlaps during leaflet separation, whereas *SALAD* expression is restricted to the leaflet margin. At P3, *SALAD* and *FveCUC2a* expression overlaps at the leaflet serration sinuses, whereas *SL1* is expressed at the serration tips.

(D) A proposed model of leaf complexity and serration regulation in *F. vesca*. *FveCUC2a* is required for both leaflet separation and serration formation at P2 and P3, respectively. Its expression is separately regulated by two transcription factors, *SL1* and *SALAD*. At the early stage when leaflets separate (P2), *SL1* positively regulates *FveCUC2a* expression and promotes leaflet separation; at the later stages when leaflet serration forms (P3), *SALAD* negatively regulates *FveCUC2a* expression to limit the serration depth.

Scale bars, 5 cm for the plants and 1 cm for the leaves in (A).

subclades of class I KNOX; they are, respectively, related to *Arabidopsis* SHOOT MERISTEMLESS (STM), BREVIPEDICELLUS (BP), and KNOTTED-LIKE FROM ARABIDOPSIS THALIANA 2/6 (KNAT2/KNAT6). Based on this analysis, FaKNOX1 is most closely to KNAT2/6 (tomato TKn4) rather than the BP (maize KN1, tomato TKn1) or STM (tomato TKn2) subclades (Figure S3). TKn4 regulates tomato meristem formation, leaf morphology, as well as fruit development but is hardly expressed in leaves.[33–35] Therefore, *FaKNOX1* may not be orthologous to the maize *KN1* or tomato *TKn2*. Future experiments overexpressing the true orthologs of maize *KN1* in strawberry may help confirm this possibility.

Alternatively, strawberry compound leaf development could be independent of *KNOXI*. We examined the expression of all six *KNOXI* genes from *F. vesca* based on prior RNA sequencing (RNA-seq) data[36,37] (Figure S4A). *FveSTMb* (GDR: FvH4_3g04270) and *FveKNOX1* (GDR: FvH4_6g07460) are most highly expressed in the receptacle meristem (REM), floral meristem (FM), and shoot apical meristem (SAM). *FveKNAT2/6La* (GDR: FvH4_5g05530) is also highly expressed in above meristem tissues plus ripening fruit (22 days turning stage fruit). The remaining three members, *FveSTMa* (GDR: FvH4_3g01400), *FveBP* (GDR: FvH4_2g32400), and *FveKNAT2/6La* (GDR: FvH4_4g26090), are all more highly expressed in the carpel wall and receptacle fruit (pith and cortex) (Figure S4A). All of them are hardly or not expressed in the young leaves (Figure S4A). Even in the young leaf primordia at P1 and P2 (plus the shoot meristem), we failed to detect any change of *FveKNAT2/6La* expression between *F. vesca* WT and *salad* mutants as well as failed to detect *FveBP* expression in WT or *salad* young leaf primordia by RT-qPCR (Figure S4B). The extremely low level of *FveKNOXI* expression in the young leaf primordia of *F. vesca* and a failure in detecting an expression difference between WT and *salad* support that strawberry leaf development may not require *KNOXI*.

Strawberry *SALAD* and its tomato homolog *CLAUSA* act differently in their respective species

The tomato *clausa* mutants dramatically increased leaf complexity by producing more than 11-fold leaflets, showed deeper leaf serrations, and formed ectopic meristems on the rachis,[27,38,39] which phenocopied the transgenic tomato overexpressing *KNOXI*

genes.[8] By contrast, the strawberry *salad* mutant does not affect leaf complexity at all. Despite this key difference, *SALAD* and *CLAUSA* are also similar in a number of ways. Both genes encode a transcriptional repressor, are expressed at the leaf margin,[26] and negatively regulate the expression of *NAM/CUC* class genes, *GOBLET* in tomato[39] and *CUC2a* in strawberry.

Although the MYB domain and EAR domain are highly conserved between SALAD and CLAUSA, other regions of the proteins are not conserved. Hence, their different phenotypes may be due to different downstream target genes. Indeed, *CLAUSA* was shown to negatively regulate *KNOXI* genes *Tkn1* and *LeT6/Tkn2*[27,38] and was also shown to attenuate cytokinin responses.[26] Hence, it appears that *CLAUSA* normally acts to attenuate meristematic activity by repressing *KNOXI* genes and dampening cytokinin responses. By contrast, our expression analysis described above indicates that *SALAD* in strawberry does not appear to regulate *KNOXI* gene expression. This is also supported by a prior RNA-seq study, which showed that none of the *KNOXI* genes was differentially expressed in *F. vesca sl1-1* mutants with reduced leaf complexity.[22] Thus, an absence of *KNOXI* expression and function in strawberry leaves may underlie *salad's* inability to impact leaf complexity.

Another contributing factor may reside in the different ways that leaf primordia develop ontogenically in these two species. The tomato leaves develop in a basipetal sequence when younger leaflets are progressively initiated closer to the base of the leaf primordium; in addition, the leaf maintains leaflet and lobe organogenesis after it has expanded.[8,9,40]In strawberry, the two flaking leaflets appear to initiate almost simultaneously as the terminal leaflet.[22] This difference in leaf ontogenesis may manifest different phenotypic outcomes in *salad* and *clausa* mutants with increased *CUC2/GOBLET* expression.

In summary, we have identified a simple mechanism in strawberry leaf development. At the early leaf developmental stages, *SL1* promotes *CUC2* expression in the rising leaf primordium to induce leaf dissection, resulting in multiple leaflets in a compound leaf. At the later stages, *SALAD* represses *CUC2* expression at the leaf margin to limit leaf margin sinus depth. This shift in upstream regulators of *CUC2* serves to coordinate and also independently control the two critical aspects of leaf morphogenesis.

STAR★METHODS

Detailed methods are provided in the online version of this paper and include the following:

- KEY RESOURCES TABLE
- RESOURCE AVAILABILITY
  - Lead contact
  - Materials availability
  - Data and code availability
- EXPERIMENTAL MODEL AND STUDY PARTICIPANT DETAILS
  - Plant materials
  - Growth conditions
- METHOD DETAILS
  - Leaf morphology analysis
  - Mapping the *salad* mutation through bulk-segregant analysis
  - Multiple sequence alignment
  - CRISPR, overexpression, and GUS constructs assembly
  - Plant transformation
  - GUS staining
  - Hormone treatment
  - RNA extraction, cDNA synthesis, and RT-qPCR
  - Phylogenetic analysis of KNOX proteins
  - Expression analysis of *KNOXI* genes
- QUANTIFICATION AND STATISTICAL ANALYSIS

SUPPLEMENTAL INFORMATION

Supplemental information can be found online at https://doi.org/10.1016/j.cub.2024.01.010.

ACKNOWLEDGMENTS

We would like to thank Dr Courtney Hollender for the EMS mutagenesis, Dr Dirk Joldersma for initially identifying the *salad* mutant, Dr Chunying Kang for the *DR5ver2:GUS* transgenic plant seeds, Dr. Yiping Qi for the CRISPR-combo system, and Dr. Harry Swartz for the *Monophylla* plant. We also thank Madison Plunkert for critical comments on the manuscript. This work has been supported by a US National Science Foundation grant (IOS1935169) to Z.L.

AUTHOR CONTRIBUTIONS

X.L. and Z.L. designed experiments; X.L., L.G., and E.T. performed experiments; Z.L. supervised and supported the project; X.L., Z.Y., and Z.L. wrote and commented on the manuscript.

DECLARATION OF INTERESTS

The authors declare no competing interests.

Received: October 25, 2023
Revised: December 19, 2023
Accepted: January 3, 2024
Published: January 24, 2024

REFERENCES

1. Nicotra, A.B., Leigh, A., Boyce, C.K., Jones, C.S., Niklas, K.J., Royer, D.L., and Tsukaya, H. (2011). The evolution and functional significance of leaf shape in the angiosperms. Funct. Plant Biol. *38*, 535–552.
2. Efroni, I., Eshed, Y., and Lifschitz, E. (2010). Morphogenesis of Simple and Compound Leaves: A Critical Review. Plant Cell *22*, 1019–1032.
3. Nikolov, L.A., Runions, A., Das Gupta, M., and Tsiantis, M. (2019). Leaf development and evolution. Chapter Five. In Current Topics in Developmental Biology Plant Development and Evolution, U. Grossniklaus, ed. (Academic Press), pp. 109–139.
4. Bharathan, G., Goliber, T.E., Moore, C., Kessler, S., Pham, T., and Sinha, N.R. (2002). Homologies in Leaf Form Inferred from KNOXI Gene Expression During Development. Science *296*, 1858–1860.
5. Shani, E., Burko, Y., Ben-Yaakov, L., Berger, Y., Amsellem, Z., Goldshmidt, A., Sharon, E., and Ori, N. (2009). Stage-Specific Regulation of Solanum lycopersicum Leaf Maturation by Class 1 KNOTTED1-LIKE HOMEOBOX Proteins. Plant Cell *21*, 3078–3092.
6. Hay, A., and Tsiantis, M. (2010). KNOX genes: versatile regulators of plant development and diversity. Development *137*, 3153–3165.
7. Hareven, D., Gutfinger, T., Parnis, A., Eshed, Y., and Lifschitz, E. (1996). The Making of a Compound Leaf: Genetic Manipulation of Leaf Architecture in Tomato. Cell *84*, 735–744.

8. Janssen, B.-J., Lund, L., and Sinha, N. (1998). Overexpression of a Homeobox Gene, LeT6, Reveals Indeterminate Features in the Tomato Compound Leaf1. Plant Physiol. *117*, 771–786.
9. Bar, M., and Ori, N. (2015). Compound leaf development in model plant species. Curr. Opin. Plant Biol. *23*, 61–69.
10. Kierzkowski, D., Runions, A., Vuolo, F., Strauss, S., Lymbouridou, R., Routier-Kierzkowska, A.L., Wilson-Sánchez, D., Jenke, H., Galinha, C., Mosca, G., et al. (2019). A Growth-Based Framework for Leaf Shape Development and Diversity. Cell *177*, 1405–1418.e17.
11. Hofer, J., Turner, L., Hellens, R., Ambrose, M., Matthews, P., Michael, A., and Ellis, N. (1997). UNIFOLIATA regulates leaf and flower morphogenesis in pea. Curr. Biol. *7*, 581–587.
12. Wang, H., Chen, J., Wen, J., Tadege, M., Li, G., Liu, Y., Mysore, K.S., Ratet, P., and Chen, R. (2008). Control of Compound Leaf Development by FLORICAULA/LEAFY Ortholog SINGLE LEAFLET1 in Medicago truncatula. Plant Physiol. *146*, 1759–1772.
13. Champagne, C.E.M., Goliber, T.E., Wojciechowski, M.F., Mei, R.W., Townsley, B.T., Wang, K., Paz, M.M., Geeta, R., and Sinha, N.R. (2007). Compound Leaf Development and Evolution in the Legumes. Plant Cell *19*, 3369–3378.
14. Aida, M., Ishida, T., Fukaki, H., Fujisawa, H., and Tasaka, M. (1997). Genes involved in organ separation in Arabidopsis: an analysis of the cup-shaped cotyledon mutant. Plant Cell *9*, 841–857.
15. Blein, T., Pulido, A., Vialette-Guiraud, A., Nikovics, K., Morin, H., Hay, A., Johansen, I.E., Tsiantis, M., and Laufs, P. (2008). A Conserved Molecular Framework for Compound Leaf Development. Science *322*, 1835–1839.
16. Bilsborough, G.D., Runions, A., Barkoulas, M., Jenkins, H.W., Hasson, A., Galinha, C., Laufs, P., Hay, A., Prusinkiewicz, P., and Tsiantis, M. (2011). Model for the regulation of Arabidopsis thaliana leaf margin development. Proc. Natl. Acad. Sci. USA *108*, 3424–3429.
17. Larue, C.T., Wen, J., and Walker, J.C. (2009). A microRNA–transcription factor module regulates lateral organ size and patterning in Arabidopsis. Plant J. *58*, 450–463.
18. Hasson, A., Plessis, A., Blein, T., Adroher, B., Grigg, S., Tsiantis, M., Boudaoud, A., Damerval, C., and Laufs, P. (2011). Evolution and diverse roles of the CUP-SHAPED COTYLEDON genes in Arabidopsis leaf development. Plant Cell *23*, 54–68.
19. Runions, A., Tsiantis, M., and Prusinkiewicz, P. (2017). A common developmental program can produce diverse leaf shapes. New Phytol. *216*, 401–418.
20. Chatterjee, M., Bermudez-Lozano, C.L., Clancy, M.A., Davis, T.M., and Folta, K.M. (2011). A Strawberry KNOX Gene Regulates Leaf, Flower and Meristem Architecture. PLoS One *6*, e24752.
21. Zhang, Y., Kan, L., Hu, S., Liu, Z., and Kang, C. (2023). Roles and evolution of four LEAFY homologs in floral patterning and leaf development in woodland strawberry. Plant Physiol. *192*, 240–255.
22. Pi, M., Zhong, R., Hu, S., Cai, Z., Plunkert, M., Zhang, W., Liu, Z., and Kang, C. (2023). A GT-1 and PKc domain-containing transcription regulator SIMPLE LEAF1 controls compound leaf development in woodland strawberry. New Phytol. *237*, 1391–1404.
23. Zheng, G., Wei, W., Li, Y., Kan, L., Wang, F., Zhang, X., Li, F., Liu, Z., and Kang, C. (2019). Conserved and novel roles of miR164-CUC2 regulatory module in specifying leaf and floral organ morphology in strawberry. New Phytol. *224*, 480–492.
24. Kincaid, D.T., and Schneider, R.B. (1983). Quantification of leaf shape with a microcomputer and Fourier transform. Can. J. Bot. *61*, 2333–2342.
25. Wachsman, G., Modliszewski, J.L., Valdes, M., and Benfey, P.N. (2017). A SIMPLE Pipeline for Mapping Point Mutations. Plant Physiol. *174*, 1307–1313.
26. Bar, M., Israeli, A., Levy, M., Ben Gera, H., Jiménez-Gómez, J.M., Kouril, S., Tarkowski, P., and Ori, N. (2016). CLAUSA Is a MYB Transcription Factor That Promotes Leaf Differentiation by Attenuating Cytokinin Signaling. Plant Cell *28*, 1602–1615.
27. Avivi, Y., Lev-Yadun, S., Morozova, N., Libs, L., Williams, L., Zhao, J., Varghese, G., and Grafi, G. (2000). Clausa, a Tomato Mutant with a Wide Range of Phenotypic Perturbations, Displays a Cell Type-Dependent Expression of the Homeobox Gene LeT6/TKn2. Plant Physiol. *124*, 541–552.
28. Aida, M., Ishida, T., and Tasaka, M. (1999). Shoot apical meristem and cotyledon formation during Arabidopsis embryogenesis: interaction among the CUP-SHAPED COTYLEDON and SHOOT MERISTEMLESS genes. Development *126*, 1563–1570.
29. Feng, J., Dai, C., Luo, H., Han, Y., Liu, Z., and Kang, C. (2019). Reporter gene expression reveals precise auxin synthesis sites during fruit and root development in wild strawberry. J. Exp. Bot. *70*, 563–574.
30. Nikovics, K., Blein, T., Peaucelle, A., Ishida, T., Morin, H., Aida, M., and Laufs, P. (2006). The Balance between the MIR164A and CUC2 Genes Controls Leaf Margin Serration in Arabidopsis. Plant Cell *18*, 2929–2945.
31. Pan, C., Li, G., Malzahn, A.A., Cheng, Y., Leyson, B., Sretenovic, S., Gurel, F., Coleman, G.D., and Qi, Y. (2022). Boosting plant genome editing with a versatile CRISPR-Combo system. Nat. Plants *8*, 513–525.
32. Challa, K.R., Rath, M., Sharma, A.N., Bajpai, A.K., Davuluri, S., Acharya, K.K., and Nath, U. (2021). Active suppression of leaflet emergence as a mechanism of simple leaf development. Nat. Plants *7*, 1264–1275.
33. Yan, F., Hu, G., Ren, Z., Deng, W., and Li, Z. (2015). Ectopic expression a tomato KNOX Gene Tkn4 affects the formation and the differentiation of meristems and vasculature. Plant Mol. Biol. *89*, 589–605.
34. Yan, F., Deng, W., Pang, X., Gao, Y., Chan, H., Zhang, Q., Hu, N., Chen, J., and Li, Z. (2019). Overexpression of the KNOX gene Tkn4 affects pollen development and confers sensitivity to gibberellin and auxin in tomato. Plant Sci. *281*, 61–71.
35. Nadakuduti, S.S., Holdsworth, W.L., Klein, C.L., and Barry, C.S. (2014). KNOX genes influence a gradient of fruit chloroplast development through regulation of GOLDEN2-LIKE expression in tomato. Plant J. *78*, 1022–1033.
36. Kang, C., Darwish, O., Geretz, A., Shahan, R., Alkharouf, N., and Liu, Z. (2013). Genome-Scale Transcriptomic Insights into Early-Stage Fruit Development in Woodland Strawberry Fragaria vesca. Plant Cell *25*, 1960–1978.
37. Li, Y., Wei, W., Feng, J., Luo, H., Pi, M., Liu, Z., and Kang, C. (2018). Genome re-annotation of the wild strawberry Fragaria vesca using extensive Illumina- and SMRT-based RNA-seq datasets. DNA Res. *25*, 61–70.
38. Jasinski, S., Kaur, H., Tattersall, A., and Tsiantis, M. (2007). Negative regulation of KNOX expression in tomato leaves. Planta *226*, 1255–1263.
39. Bar, M., Ben-Herzel, O., Kohay, H., Shtein, I., and Ori, N. (2015). CLAUSA restricts tomato leaf morphogenesis and GOBLET expression. Plant J. *83*, 888–902.
40. Burko, Y., and Ori, N. (2013). The Tomato Leaf as a Model System for Organogenesis. In Plant Organogenesis: Methods and Protocols Methods in Molecular Biology, I. De Smet, ed. (Humana Press), pp. 1–19.
41. Slovin, J.P., Schmitt, K., and Folta, K.M. (2009). An inbred line of the diploid strawberry Fragaria vesca f. semperflorens for genomic and molecular genetic studies in the Rosaceae. Plant Methods *5*, 15.
42. Hawkins, C., Caruana, J., Schiksnis, E., and Liu, Z. (2016). Genome-scale DNA variant analysis and functional validation of a SNP underlying yellow fruit color in wild strawberry. Sci. Rep. *6*, 29017.
43. Caruana, J.C., Sittmann, J.W., Wang, W., and Liu, Z. (2018). Suppressor of Runnerless Encodes a DELLA Protein that Controls Runner Formation for Asexual Reproduction in Strawberry. Mol. Plant *11*, 230–233.
44. Chen, S., Zhou, Y., Chen, Y., and Gu, J. (2018). fastp: an ultra-fast all-in-one FASTQ preprocessor. Bioinformatics *34*, i884–i890.
45. Edger, P.P., VanBuren, R., Colle, M., Poorten, T.J., Wai, C.M., Niederhuth, C.E., Alger, E.I., Ou, S., Acharya, C.B., Wang, J., et al. (2018). Single-molecule sequencing and optical mapping yields an improved genome of woodland strawberry (Fragaria vesca) with chromosome-scale contiguity. GigaScience *7*, 1–7.
46. Li, Y., Pi, M., Gao, Q., Liu, Z., and Kang, C. (2019). Updated annotation of the wild strawberry Fragaria vesca V4 genome. Hortic. Res. *6*, 61.

47. Zhou, J., Wang, G., and Liu, Z. (2018). Efficient genome editing of wild strawberry genes, vector development and validation. Plant Biotechnol. J. *16*, 1868–1877.

48. Zhou, J., Sittmann, J., Guo, L., Xiao, Y., Huang, X., Pulapaka, A., and Liu, Z. (2021). Gibberellin and auxin signaling genes RGA1 and ARF8 repress accessory fruit initiation in diploid strawberry. Plant Physiol. *185*, 1059–1075.

49. Curtis, M.D., and Grossniklaus, U. (2003). A gateway cloning vector set for high-throughput functional analysis of genes in planta. Plant Physiol. *133*, 462–469.

50. Guo, L., Luo, X., Li, M., Joldersma, D., Plunkert, M., and Liu, Z. (2022). Mechanism of fertilization-induced auxin synthesis in the endosperm for seed and fruit development. Nat. Commun. *13*, 3985.

51. Clough, S.J., and Bent, A.F. (1998). Floral dip: a simplified method for Agrobacterium-mediated transformation of Arabidopsis thaliana. Plant J. *16*, 735–743.

52. Kurihara, D., Mizuta, Y., Sato, Y., and Higashiyama, T. (2015). ClearSee: a rapid optical clearing reagent for whole-plant fluorescence imaging. Development *142*, 4168–4179.

53. Vandesompele, J., De Preter, K., Pattyn, F., Poppe, B., Van Roy, N., De Paepe, A., and Speleman, F. (2002). Accurate normalization of real-time quantitative RT-PCR data by geometric averaging of multiple internal control genes. Genome Biol. *3*. RESEARCH0034.

54. Lu, R., Pi, M., Liu, Z., and Kang, C. (2023). Auxin biosynthesis gene FveYUC4 is critical for leaf and flower morphogenesis in woodland strawberry. Plant J. *115*, 1428–1442.

STAR★METHODS

KEY RESOURCES TABLE

REAGENT or RESOURCE	SOURCE	IDENTIFIER
Bacterial and virus strains		
E. coli	Widely distributed	10β
Agrobacterium tumefaciens	Widely distributed	GV3101
Chemicals, peptides, and recombinant proteins		
Murashige & Skoog medium with Gamborgs's B5 Vitamins	Research Products International	Cat. #M10500
Sucrose	Fisher Bioreagents	Cat. #BP220-1
Dextrose anhydrous	Fisher Bioreagents	Cat. #D19-212
6-Benzylaminopurine	Sigma-Aldrich	Cat. #B-3408
Indole-3-butyric acid	Sigma-Aldrich	Cat. #I5386
Phyto Agar	Research Products International	Cat. #A20300
Timentin™ Ticarcillin/Clavulanate(15:1)	Gold Biotechnology	Cat. #T-104
Carbenicillin (Disodium)	Gold Biotechnology	Cat. #C-103
Hygromycin B	Gold Biotechnology	Cat. #H-270
X-gluc (CHX salt)	Gold Biotechnology	Cat. #G1281
EDTA Disodium Salt	Fisher Bioreagents	Cat. #BP120
Triton X-100	Promega	Cat. #H5141
Potassium ferricyanide	Sigma-Aldrich	Cat. #702587
Potassium ferrocyanide	Sigma-Aldrich	Cat. #P3289
Xylitol	Sigma-Aldrich	Cat. #X3375
Sodium deoxycholate	Sigma-Aldrich	Cat. #D6750
Urea	Ambion	Cat. #9902
1-Naphthaleneacetic acid	Sigma-Aldrich	Cat. #N0640
N-1-naphthylpthalamic acid (NPA)	Phyto Technology Laboratory	Cat. #N6250
Critical commercial assays		
DNeasy® PowerPlant® Pro kit	Qiagen	Cat. #13400-50
NucleoSpin® Plant II kit	Macherey-Nagel	Cat. #740770.50
NucleoSpin® gDNA Clean-up kit	Macherey-Nagel	Cat. # 740230.50
Monarch® Total RNA Miniprep kit	New England Biolabs	Cat. #T2010S
RevertAid™ First Strand cDNA Synthesis Kit	Thermo Scientific	Cat. #K1622
PowerUp SYBR Green Master Mix	Applied Biosystem	Cat. #A25742
AccuStart™ II PCR ToughMix	QuantaBio	Cat. #95142-800
NGS sequencing, NovaSeq 6000	Novogene	N/A
CFX96 Real Time System	Bio-Rad	N/A
Dual-Luciferase® Reporter Assay System	Promega	Cat. #E1910
Gateway™ LR Clonase™ II Enzyme mix	Invitrogen	Cat. #11791020
Canon G12 camera	Canon	N/A
Nikon Eclipse E600 microscope	Nikon	N/A
Nikon SMZ1000 stereomicroscope	Nikon	N/A
Q5®High-Fideligy DNA Polymerase	New England Biolabs	Cat. #M0491L
Deposited data		
Whole genome resequencing data of WT bulk and *salad* bulk	This study	SRA: BioProject PRJNA1019070
Experimental models: Organisms/strains		
F. vesca; 'Yellow Wonder' 5AF7	Slovin et al.[41]	YW5AF7
F. vesca; 'Hawaii4'	Hawkins et al.[42]	#PI551572

(*Continued on next page*)

Continued		
REAGENT or RESOURCE	SOURCE	IDENTIFIER
F. vesca; '*monophylla*'	Pi et al.[22]	Strawberry of Versailles
F. vesca; *fvecuc2a-2* mutant	Zheng et al.[23]	N/A
F. vesca; *salad* mutant	This study	N/A
F. vesca; SALADpro::GUS in YW5AF7	This study	N/A
F. vesca; *FveCUC2apro::GUS* in YW5AF7	This study	N/A
F. vesca; DR5ver2::GUS in YW5AF7	This study	N/A
A. thaliana; Col-0	Widely distributed	N/A
A. thaliana; *atsalad*^{CR} in Col-0	This study	N/A
Oligonucleotides		
Primers used in this study	This study, Table S2	N/A
Recombinant DNA		
JH19-SALADg1g2	This study	N/A
JH23-FveSALAD	This study	N/A
pMDC162-SALADpro::GUS	This study	N/A
pMDC162-CUC2apro::GUS	This study	N/A
JH23-AtSALAD CRISPR combo	This study	N/A
Software and algorithms		
Image J (1.53k)	National Institutes of Health, USA	http://imagej.nih.gov/ij
GraphPad Prism (V10.0.3)	GraphPad Software, Boston, MassachusettsUSA	https://www.graphpad.com/
Clustral Omega	EMBL-EBL	https://www.ebi.ac.uk/Tools/msa/clustalo/
MEGA X	MEGA Software	https://www.megasoftware.net/
SIMPLE pipeline	Wachsman et al.[25]	https://github.com/wacguy/Simple
R	R core team	https://www.r-project.org/
Protein Blast	NCBI	https://blast.ncbi.nlm.nih.gov/Blast.cgi

RESOURCE AVAILABILITY

Lead contact

Further information and requests for resources and reagents should be directed to and will be fulfilled by the lead contact, Zhongchi Liu (zliu@umd.edu).

Materials availability

The plasmids and genetic materials generated in this study are available from the corresponding authors upon request.

Data and code availability

- The genome resequencing data used for mapping the *salad* mutation have been deposited at NCBI Sequence Read Archive (SRA) and are publicly available as of the date of publication. Project numbers are listed in the key resources table.
- This paper does not report original code.
- Any additional information required to reanalyze the data reported in this paper is available from the lead contact upon request.

EXPERIMENTAL MODEL AND STUDY PARTICIPANT DETAILS

Plant materials

The seventh-generation inbred line of *F. vesca* accession Yellow Wonder 5AF7 (YW5AF7)[41,42] was used as the wild type in this study. The *salad* mutant was identified in the M2 generation of an Ethyl methane sulfonate (EMS) mutagenesis screen in the YW5AF7 background. The mutagenesis was previously described.[43] *fvecuc2a-2* was identified in a previous ENU mutagenesis screen in YW5AF7.[23] DR5ver2::GUS (in YW5AF7) seeds were from Dr. Chunying Kang.[29] *F. vesca* cultivar *Monophylla* ('Strawberry of Versailles') was gifted to us by Dr. Harry Swartz. Wild strawberry transgenic lines were generated in YW5AF7 background and *Arabidopsis thaliana* transgenic lines were generated in Col-0 background.

Growth conditions

The plants grown in soil were cultivated in a growth chamber under white light, provided by Phillips F32T8/TL841 linear fluorescent bulbs, with light intensity of 110 μmol m^{-2} s^{-1} and a 13/11 h light/dark photoperiod at 22 °C. For tissue culture and in hormone treatment experiments, calli or plants were grown in vitro on MS medium with or without supplements in petri dishes or Magenta tissue culture vessels in a growth camber with light intensity of 80 μmol m^{-2} s^{-1} and a 16/8 h light/dark photoperiod at 22 °C.

METHOD DETAILS

Leaf morphology analysis

Fifteen mature leaves from five plants (three leaves per individual) were used to quantify leaf serration numbers and leaf dissection index. For leaf serration number measurement, serrations were counted and documented for each leaflet. For leaf index measurement, mature leaves were cut off and taped onto a blank paper, and then scanned into digital image. ImageJ software was used to extract the terminal leaflets and quantify their area and perimeter. The leaf dissection index was calculated using the formula $LDI = \frac{perimeter}{2\sqrt{area \times \pi}}$, where values are relative to a circle which has a LDI of 1.[24] Student's t-test (****, $P < 0.0001$) was performed using the Graphpad Prism version 10.0.3 software.

Mapping the *salad* mutation through bulk-segregant analysis

The *salad* mutant was crossed with *F. vesca* accession 'Hawaii 4 (H4)' to produce the F_2 mapping population. Leaf morphology was scored in the F2 population, and genomic DNA was pooled from 25 mutant and 25 wild-type individuals respectively. Genomic DNA was extracted with DNeasy PowerPlant Pro kit (Qiagen, USA) or NucleoSpin Plant II kit (Macherey-Nagel, USA), followed by cleanup with the NucleoSpin Genomic DNA Cleanup kit (Macherey-Nagel, USA). The two DNA pools were sequenced using the Illumina NovaSeq 6000 System (Novogene, Sacramento, USA).

A total of 118.4 and 112.5 million paired-end 150 bp reads respectively from *salad* and wild-type were filtered using fastp[44] to remove low quality reads. Candidate *salad* mutations were identified using the SIMPLE pipeline.[25] Briefly, SIMPLE maps sequencing reads to the *F. vesca* reference genome,[45,46] calls SNPs between the mutant and wild type bulks, plots the ratio between the proportion of reference reads in the wild-type bulk and the proportion of reference reads in the mutant bulk (Figure S1), and identifies candidate SNPs expected to affect gene function. Known variants occurring in the accessions YW5AF7 and H4 were filtered out. SNPs that are expected to affect gene function as a missense, nonsense, or splicing variant not known to occur in YW5AF7 or H4 genome were selected as candidates (Table S1).

Multiple sequence alignment

SALAD homolog genes in *Arabidopsis thaliana* and tomato (*Solanum lycopersicum*) were identified by Protein Blast (https://blast.ncbi.nlm.nih.gov/Blast.cgi) using *F. vesca* SALAD full length protein sequence as query, the first hits were identified as homologs. The protein sequences were downloaded from The Arabidopsis Information Resource (TAIR, https://www.arabidopsis.org/) and the Sol Genomics Network (SGN, https://solgenomics.net/). Multiple sequence alignment was created using the Clustal Omega program by default settings hosted on EMBL-EBL (https://www.ebi.ac.uk/Tools/msa/clustalo/).

CRISPR, overexpression, and GUS constructs assembly

Genomic DNA or cDNA extracted from young leaves of YW5AF7 was used for sequence amplification. All primers used are listed in Table S2.

To assemble the JH19-SALADg1g2 construct, gRNA1 (GATCCAAGGTGCCTCGTCTG) and gRNA2 (GATGTTTAGAAGCATGAGGGG) targeting the coding region of *SALAD* were inserted into the JH4 entry vector and then incorporated into the binary vector JH19 via gateway cloning.[47] To confirm editing in the hygromycin-resistant seedlings, genomic sequences spanning the target site of respective genes were amplified by PCR and analyzed by Sanger sequencing. Five lines were obtained with different types of editing.

To assemble JH23-FveSALAD vector, the coding region of *FveSALAD* was cloned form YW5AF7 cDNA and Gibson-assembled in to the JH23 vector[48] following K*pn*I and P*ac*I digestion. Following floral dipping transformation in Arabidopsis Col-0, progeny seeds were selected with hygromycin (30 μg/ml) antibiotics.

To assemble pMDC162-SALADpro::GUS and pMDC162-CUC2apro::GUS vectors, the promoter of *SALAD* (2154 bp upstream of the start codon) and *FveCUC2a* (2004 bp upstream of the start codon) were cloned from YW5AF7 genomic DNA respectively and assembled into the pMDC162 vector.[49] To confirm the transgene in the hygromycin positive seedlings, the GUS gene was amplified by PCR using YW5AF7 as the negative control.

The JH23-AtSALAD CRISPR combo construct was cloned as described in the Cas9-Act3.0 system,[31] where *AtFT* was activated simultaneously to accelerate the flowering along with editing of the two *SALAD* homologs in Arabidopsis. Briefly, six synthesized gRNA oligos were phosphorylated and annealed before ligated to gRNA expression vectors digested by B*sm*BI. Specifically, four 18 nt gRNAs targeting AT1G14600 and AT2G02060 coding regions for gene editing were ligated to the vectors pYPQ131-134, two 15 nt gRNAs targeting *AtFT* promoter for gene activation were ligated to vectors pYPQ131B-132B. Then six gRNA expression

vectors were ligated into the pYPQ146 vector digested by BsaI. Finally, Gateway LR reaction was carried out using the Cas0-Act3.0 entry vector, pYPQ146gRNAs vector and destination vector JH23 to clone the gRNAs into the binary vector JH23. Sanger sequencing was used to validate the constructs.

Plant transformation

Agrobacterium-mediated transformation in woodland strawberry was carried out as previously described with minor modification.[50] Briefly, cotyledons or juvenile simple leaves of YW5AF7 seedlings grown on MS medium were cut and vacuum infiltrated with *Agrobacterium tumerfaciens* strain GV3101 containing a CRISPR/Cas9 or GUS expression construct using a syringe barrel and plunger. The infected explants were kept on the 5 ++ medium (1 × MS, 2% sucrose, 3.4 mg/L benzyl adenine, 0.3 mg/L indole-3-butyric acid (IBA), 0.7% phytoagar, pH 5.8) for three days in the dark, then washed with sterile water and put onto the MS medium with antibiotics (250 mg/L Timentin + 250 mg/L Carbenicillin). The explants were then kept under dark for seven days to induce calli. Transformed calli were selected on the 5++ medium with 250 mg/L Timentin, 250 mg/L Carbenicillin and 4 mg/L Hygromycin. The calli were moved to fresh medium (5++ medium with the same three antibiotics) every 2-3 weeks until shoots appear in a growth chamber. When the shoots grew larger, they were transferred to the rooting medium (0.5 x MS, 0.01 mg/L IBA, 2% glucose, 0.7% phytoagar, pH 5.8) with 4 mg/L Hygromycin. After about 1–2 months, the plants with roots were transferred to soil and genotyped.

Arabidopsis Col-0 plants were transformed through floral dipping method,[51] using *Agrobacterium tumerfaciens* strain GV3101 containing the JH23-AtSALAD CRISPR combo construct.

GUS staining

GUS staining was carried out as previously reported.[22] The shoot apices of the *SALADpro::GUS* and *CUC2apro::GUS* transgenic lines in T0 were collected and applied to GUS staining in the buffer (1 mM X-glucuronic acid, 0.1 mM EDTA, 0.1% Triton X-100, and 10 mM potassium ferri/ferrocyanide in 100 mM phosphate buffer, pH 7.0). After 30 min of vacuum infiltration, tissues were incubated at 37°C for 2–5 hr. The shoot apices of *DR5ver2::GUS* transgenic lines in wildtype and *salad* background were collected and applied to GUS staining in the buffer containing 2 mM potassium ferri/ferrocyanide, and incubated at 37°C overnight after vacuum infiltration. The samples were then treated in the ClearSee solution [10% (w/v) xylitol, 15% (w/v) sodium deoxycholate, 25% (w/v) urea dissolved in water][52] for 2-4 days until the chlorophyll was cleared. Samples were observed under Nikon Eclipse E600 microscope with DIC or Nikon SMZ1000 stereomicroscope with a LED light source from the bottom. Images were taken with a SPOT RT KE Color Mosaic Camera or a Nikon Digital camera DXM1200 attached to the scopes.

Hormone treatment

YW5AF7 and *salad* were germinated and grown on MS medium w. 2% sucrose for 1 month before seedlings were transferred to MS medium with 2% sucrose with or without NAA (1 μM) or NPA (20 μM) in the Magenta tissue culture vessels for 1 month. Leaves of the seedlings were photographed with a Canon G12 camera.

RNA extraction, cDNA synthesis, and RT-qPCR

Total RNA was extracted from young leaves of developmental stages of interest. 10–20 leaves sampled from at least three individuals were pooled to form one biological replicate, and three biological replicates were used. Tissues were flash-frozen in liquid nitrogen immediately after collection and stored at -80 °C until RNA extraction. RNA was extracted using Monarch Total RNA Miniprep kit. RNA was reverse transcribed to cDNA using RevertAid First Strand cDNA Synthesis Kit, and RT-qPCR was performed using the Bio-Rad CFX96 Real-time system and PowerUp SYBR Green Master Mix, using a three-step PCR program (step 1, 50°C, 2 min; step 2, 95 °C, 2 min; step 3, 95 °C, 15 s; step 4, 55 °C, 15 s; step 5, 72 °C, 30 s; repeat steps 3–5, 40 cycles). The relative expression level was analyzed using a modified $2^{-\Delta\Delta CT}$ method normalized to the geometric mean of the CT value of the two internal controls.[53] For genes whose transcripts were undetectable by RT-qPCR, the cycle number was set to 40 for calculation as only 40 cycles were performed for all PCR reactions. For all RT-qPCRs, *F. vesca Protein Phosphatase 2A* (*FvePP2a*; FvH4_4g27700) were used as the internal controls.[48,50,54] Primers are listed in Table S2.

Phylogenetic analysis of KNOX proteins

KNOX protein sequences in *F. vesca*, *F.* × *ananassa*, *Arabidopsis*, tomato, and Maize were downloaded from Genome Database for Rosaceae (GDR, https://www.rosaceae.org/), TAIR, the Sol Genomics Network and NCBI. A multiple sequence alignment containing these sequences, as well as *Arabidopsis* BEL1 as an outgroup, was created using the MUSCLE algorithm implemented in MEGA X software (https://www.megasoftware.net/). The rooted maximum likelihood phylogeny tree was constructed with 1000 bootstrap replicates (Figure S3).

Expression analysis of *KNOXI* genes

F. vesca KNOXI genes were identified by blast against *F. vesca* genome v4.0.a1 using *Arabidopsis KNOXI* genes (*STM* / AT1G62360, BP / AT4G08150, AtKNAT2 / AT1G70510, AtKNAT6 / AT1G23380) at the GDR website. Expression levels of *KNOXI* genes in different tissues of *F. vesca* were retrieved from a prior study represented[37] and visualized with a hierarchical clustering heatmap (Figure S4) using the website ClustVis (https://biit.cs.ut.ee/clustvis/).

QUANTIFICATION AND STATISTICAL ANALYSIS

Statistical analyses and visualization were performed using GraphPad Prism version 10.0.3 for Windows, GraphPad Software, Boston, Massachusetts USA (www.graphpad.com). Pairwise comparisons were performed using Student's t-test. Multiple comparisons were performed using multiple unpaired *t* test corrected by FDR method.